



## RESEARCH ARTICLE

# Branched plasticizers derived from eugenol via green polymerization for low/non-migration and externally/internally plasticized polyvinyl chloride materials



Yun Hu <sup>a,1</sup>, Jing Zhou <sup>c,1</sup>, Yufeng Ma <sup>b</sup>, Yu Bei <sup>b,d</sup>, Feilong Hu <sup>e</sup>, Zhimin Kou <sup>a,b</sup>, Yonghong Zhou <sup>a,d</sup>, Puyou Jia <sup>a,\*</sup>

<sup>a</sup> Institute of Chemical Industry of Forest Products, Chinese Academy of Forestry (CAF), Jiangsu Key Lab of Biomass Energy and Materials, Jiangsu Province, 16 Suojin North Road, Nanjing 210042, China

<sup>b</sup> College of Materials Science and Engineering, Co-Innovation Center of Efficient Processing and Utilization of Forest Resources, Nanjing Forestry University, 159 Longpan Road, Nanjing 210037, China

<sup>c</sup> Weifang Vocational College, School of Chemical Engineering, 06588 Hai'an Road, Weifang 262737, Shandong, China

<sup>d</sup> College of Chemical Engineering, Nanjing Forestry University, Nanjing 210037, China

<sup>e</sup> Key Laboratory of Chemistry and Engineering of Forest Products, State Ethnic Affairs Commission, Guangxi Key Laboratory of Chemistry and Engineering of Forest Products, Guangxi Minzu University, Nanning 530006, China

Received 6 June 2022; accepted 3 October 2022

Available online 10 October 2022

## KEYWORDS

Waste residues of the rosin processing industry;  
Eugenol;  
Sustainable plasticizer;  
Green polymerization

**Abstract** The synthesis of nontoxic plasticizers derived from the waste residues of the rosin-processing industry can reduce pollution and promote the high-value utilization of the waste residues of rosin. In this study, four kinds of sustainable branched plasticizers derived from a biomass resource, eugenol (derived from the waste residues of the rosin processing industry), were synthesized via one-pot solvent free polymerization and used to plasticize polyvinyl chloride (PVC). Internally plasticized PVC was fabricated using thiolated DPE (branched plasticizers based on eugenol). The thermal stability, tensile properties, microstructure, volatility behavior, and solvent extraction resistance of plasticized PVC were investigated. Compared with the behavior of the commercial plasticizer dioctyl phthalate, the thermal stability, plasticizing efficiency, and migration resistance of the branched plasticizers are superior. The acute oral toxicity dose of each branched plasticizer was extremely high at 5000 mg/kg of body weight, with no deaths among test animals. Compared

\* Corresponding author.

E-mail address: [jiapuyou@icifp.cn](mailto:jiapuyou@icifp.cn) (P. Jia).

<sup>1</sup> These authors contributed equally to this work.

Peer review under responsibility of King Saud University.



with externally plasticized PVC, the internally plasticized PVC showed zero weight loss in volatility and leaching tests despite its less effective plasticization. All the branched plasticizers have potential application in plastic products.

© 2022 The Authors. Published by Elsevier B.V. on behalf of King Saud University. This is an open access article under the CC BY-NC-ND license (<http://creativecommons.org/licenses/by-nc-nd/4.0/>).

## 1. Introduction

Owing to the increasing shortages in petroleum resources, the development of environmentally friendly, efficient and migration-resistant bio-based plasticizers have gradually become of major interest in the plasticizer industry (Kan et al., 2020). As early as the 19th century, natural camphor balls and castor oil were used to plasticize celluloid or celluloid paint. At the beginning of the 20th century, camphor pills were gradually replaced by triphenyl phosphate. The application of ester plasticizers represents an extremely important milestone in the history of plasticizer development. By 1968, a total of 550 plasticizers had been commercialized (Wilkes et al., 2005). However, only 60 are actually used. In the past 10 years, the annual production of plasticizers in the world has been approximately 6.4 million tons. The production in Europe, North America, and Asia is 1 million tons, 800,000 tons, and 3.5 million tons, respectively. The global demand for plasticizers reached 13.2 million tons per year in 2018 (Ji et al., 2019). Therefore, green new materials are needed to meet the growing demand for nontoxic, nonmigrating, and sustainable plasticizer.

Biobased plasticizers can be derived from various agricultural products, are sustainable and abundantly available, and have low costs. Plant oil from soybean, flaxseed, palm, castor, and other plants can be directly prepared or obtained through chemical modification (Mukherjee and Ghosh, 2020; He et al., 2019; Hu et al., 2018; Xuan et al., 2019; Sinisi et al., 2019; Zhu et al., 2021). Starch and cellulose obtained from wheat, corn, rice, or potato can be used in preparing various sugar derivatives (such as mannose, glucose, fructose, sorbitol, xylitol, sorbitol, and mannitol), which are indispensable raw materials for synthesizing sugar-based plasticizers (Antti et al., 2018). Citric acid can be extracted from sugarcane, beet root, or lemon. It is an attractive raw material for generating biobased plasticizers and can be used in the synthesis of various kinds of citric acid or acetylcitrate plasticizers (Xu and Gye, 2018). The excellent plasticization of hyperbranched oligomers has been recognized, and hyperbranched oligomers derived from the biomonomers, glycerol, and adipic acid are unusually effective (Howell and Lazar, 2019).

Rosin is one of the most important sustainable resources in the forest chemical industry; it is derived from pine trees and widely used in the field of papermaking, coating, and dyeing due to its excellent anticorrosion and insulation properties, abundance in nature, and low cost (Fu-Lan and Yan, 2011; Demircan et al., 2020; Luo et al., 2012). However, large amounts of waste residues, such as pine tar and black rosin, are produced during the production of rosin-refining products, as shown in Fig. 1. Pine tar and black rosin contain many phenolic chemicals, such as eugenol, which can be obtained through the distillation of waste residues (Nagai et al., 1977). Eugenol is a potential material for constructing functional chemicals and polymer materials because of its low toxicity and renewable nature (Harvey et al., 2014; Jianping et al., 2015). It is used in the synthesis of biobased polymers, such as epoxy resins (Wan et al., 2016); cyanate esters (Harvey et al., 2015), benzoxazine (Dumas et al., 2015) and polycarbonate (Trita et al., 2017).

Herein, sustainable branched plasticizers based on the distillation product of waste residues from the rosin-processing industry (eugenol) have been synthesized via green polymerization. Specifically, eugenol with flexible aliphatic units and conterminous acid and hyperbranched ester functionality has been used for generating branched plasticizers. These materials may interact with PVC through intermolecular forces and improve mechanical properties, particularly increasing elongation

at break and lowering tensile strength. The thermal stability, tensile properties, microstructure, volatility behavior, and solvent extraction resistance of PVC with these materials have been investigated.

## 2. Materials and methods

### 2.1. Materials

Eugenol, glycidol, sodium methoxide, acetic anhydride, azodiisobutyronitrile (AIBN), chloroform, 3,6-Dioxa-1,8-octanedithiol, ethyl acetate, trimethylolpropane tris(3-mercaptopropionate), sodium hydroxide, magnesium sulphate, tetrahydrofuran (THF), pentaerythritol tetra(3-mercaptopropionate) were purchased from Shanghai Aladdin Biochemical Technology Co., Ltd, China. PVC(KM-31) was provided by Hanwha Chemical Corporation.

### 2.2. Synthesis of branched polyols based on eugenol (HPE) and branched plasticizers based on eugenol (DPE)

Eugenol (30 g, 0.18 mol) was put in a reaction vessel filled with nitrogen. Glycidol (53.2 g, 0.72 mmol) was dropped in the reaction vessel by an injection pump. When all glycidol was added in the reaction vessel in 3.5 h, the temperature was kept at 100 °C for 3.5 h to finish the reaction. HPE was obtained for characterization. Excess acetic anhydride was added in the reaction vessel. The temperature was kept at 130 °C. The mixture was stirred for 4 h to complete the reaction. DPE were obtained after purification. The synthesis scheme for HPE and DPE production are shown Fig. S1.

### 2.3. Synthesis of dimeric (DDPE), trimeric (DTPE), and tetrameric (DTDPE) branched plasticizer based on eugenol

DPE (10 g, 14.2 mmol), 3,6-dioxa-1,8-octanedithiol (1.30 g, 7.1 mmol) and AIBN (0.1 g) were dissolved in THF. The mixture was added in a reaction vessel filled with nitrogen. Then, the reaction was kept at 65 °C for night. The product was diluted with dichloromethane and washed with DI water. The organic filtrate was removing to obtain DDPE. DTPE and DTDPE were prepared using the similar reaction process. When the thiol intermediates were trimethylolpropane tris(3-mercaptopropionate) and pentaerythritol tetra(3-mercaptopropionate), the mole ratios of DPE and thiol intermediates were 3:1 and 4:1, respectively, the mass of AIBN was 1 wt% of DPE, and the obtained products were DTPE and DTDPE. The synthetic scheme is shown in Fig. S1.

### 2.4. Synthesis of thiolated DPE(DPE-SH) and DPE sodium mercaptan (DPE-SNa)

DPE (10 g, 14.2 mmol), 3,6-dioxa-1,8-octanedithiol (2.58 g, 14.2 mmol), and AIBN (0.1 g) were dissolved in THF. The

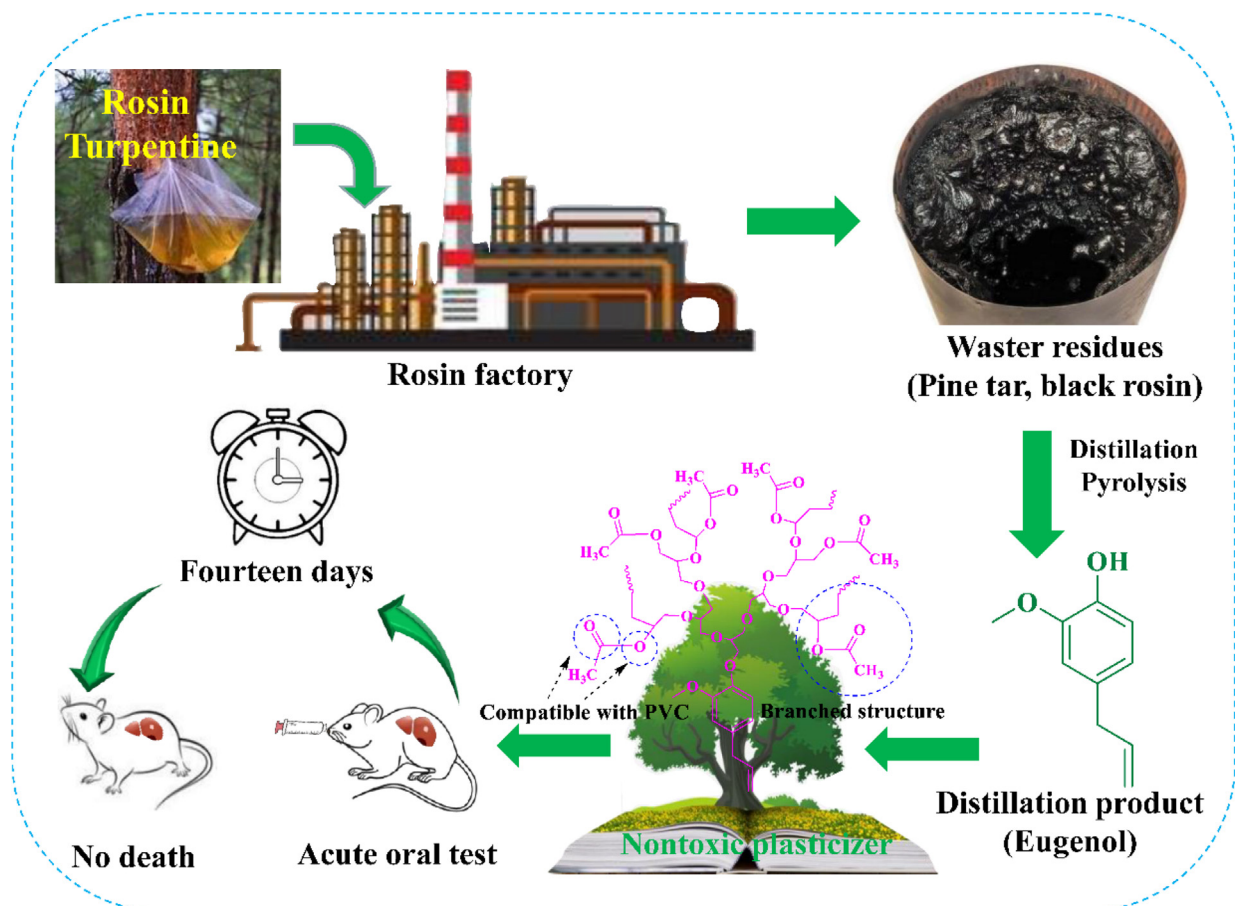


Fig. 1 Synthesis scheme route of eugenol using the rosin residue.

mixture was equipped in a reaction vessel filled with nitrogen. The temperature was kept at 65 °C. The reaction was finished after stirring for night. The products were diluted in dichloromethane and washed with brine solution. The filtrate from organic layer was distilled to obtain DPE-SH. DPE-SH and sodium methoxide in a mole ratio of 1:1 was dissolved in methanol under nitrogen atmosphere. The mixture was stirred at 60 °C for 12 h. Then, we removed methanol through distillation at reduced pressure for the production of crude product. DPE-SNa was obtained after washing with petroleum ether, filtration, and drying for the removal of petroleum ether. The synthetic route is shown in Fig. S2.

### 2.5. Synthesis of internally plasticized PVC

PVC (1 g, 0.012 mmol) and DPE-SNa (0.4 g, 0.441 mmol) were mixed together using THF as solvent under nitrogen atmosphere. The mixture was kept stirring at 60 °C for night. The internally plasticized PVC was obtained after precipitation in methanol and water ( $v/v = 1:1$ ) and dried in an oven at 50 °C for 36 h. The internally plasticized PVC was named as

PVC-40 wt% DPE-SNa. When the mass of DPE-SNa was 0.8 g, the obtained internally plasticized PVC was named as PVC-80 wt% DPE-SNa.

### 2.6. Preparation of plasticized PVC films

PVC and DDPE was dissolved in THF to obtain transparent solution. The mass ratio of PVC and DDPE is 5:2. Then, the solution was poured in a glass-surface vessel. Plasticized PVC films were prepared after removing THF. Plasticized PVC with DPE, DDPE, DTDPE, and DTPE were labeled as PVC 40 wt% DPE, PVC 40 wt% DDPE, PVC 40 wt% DTPE, and PVC 40 wt% DTDPE, respectively. Internally plasticized PVC films were prepared without adding any plasticizer according to similar process.

### 2.7. Characterization

Acute oral toxicity test, Fourier transform infrared (FT-IR) spectroscopy, <sup>1</sup>H nuclear magnetic resonance (<sup>1</sup>H NMR), thermogravimetric analysis (TGA), differential scanning

calorimetry, tensile tests, surface morphology, and atomic force microscopy (AFM) were performed, migration resistance was investigated. The methods are provided in [Supporting Information](#).

### 3. Results and discussion

#### 3.1. The structure of plasticizers

DPE was prepared through one-pot solvent-free reaction derived from eugenol, as shown in [Fig. S1](#). HPE was the intermediate product during the reaction, the feed ratio of glycidol to eugenol was adjusted to 4:1, and DPE was synthesized from HPE and acetic anhydride. Eugenol and the intermediate products HPE and DPE were characterized in [Fig. 2](#). As shown in [Fig. 2\(a\)](#), the peak at  $3532\text{ cm}^{-1}$  in the FT-IR spectrum of eugenol was attributed to  $\text{—OH}$ . The peak at  $1601\text{ cm}^{-1}$  was assigned to  $\text{C=C}$ . Compared with eugenol, the absorption peak ( $\text{—OH}$ ) at  $3377\text{ cm}^{-1}$  was stronger than eugenol, indicating that more  $\text{—OH}$  was chemically linked to alkane chain of HPE. No peak was detected at approximately  $3377\text{ cm}^{-1}$  in the FT-IR spectrum of DPE, and a strong infrared absorption peak appeared at  $1735\text{ cm}^{-1}$  attributing to  $\text{C=O}$ . The results illustrated the esterification was completed,

and DPE was obtained. HPE and DPE were investigated through  $^1\text{H}$  NMR, as shown in [Fig. 3\(a\)](#). The peaks at 6.50–6.75 ppm were assigned to the protons of benzene ring from eugenol, and the peak at 5.78 ppm was attributed to the protons of  $\text{—CH=CH—}$  (Silva et al., 2018; Teixeira et al., 2018; Faye et al., 2017; Hu et al., 2017). New peaks appeared at 3.81–4.12 ppm, which were attributed to the protons of the methyl groups of HPE, which connected to the ether bond in glycidol. The new peak at approximately 3.4 ppm was assigned to the protons of methylene groups linked to hydroxyl group, indicating that more  $\text{—OH}$  appeared on the main chains of HPE (Song et al., 2020; Ma et al., 2020; Won et al., 2018; Huang et al., 2018).  $^1\text{H}$  NMR of DPE was similar to that of HPE, but a new and strong peak appeared at 0.9 ppm, which corresponded to the protons of methyl groups, indicating that the esterification was completed.

DDPE, DTPE, and DTDPE were synthesized through thiol-ene click reaction. The infrared characteristic absorption peaks of olefins were observed at  $1610\text{ cm}^{-1}$  in the FT-IR spectrum of DPE, as shown in [Fig. 2\(a\)](#), but no peak was detected at  $1610\text{ cm}^{-1}$  in the FT-IR spectra of DDPE, DTDPE, and DTPE ([Fig. 2\(b\)](#)). The strong characteristic absorption peak of the carbonyl group at  $1733\text{ cm}^{-1}$  indicated that the thiol-ene click reaction was completed. The peak at 5.78 ppm in the  $^1\text{H}$  NMR spectrum of DPE was attributed to the protons

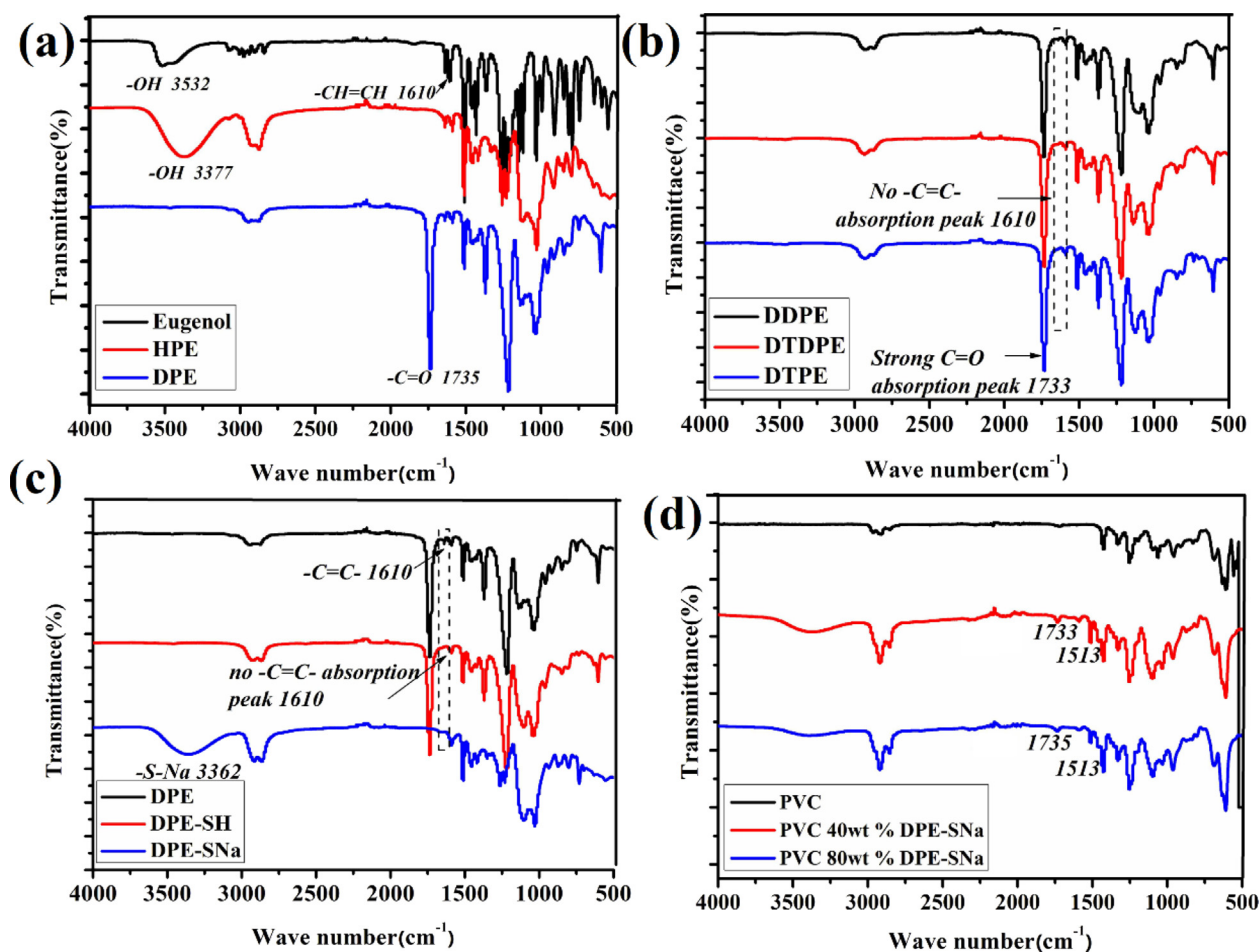


**Fig. 2** (a) FT-IR spectra of eugenol, HEP and DPE (b) FT-IR spectra of DDPE, DTPE and DTDPE (c) FT-IR spectra of DEP, DPE-SH and DPE-SNa (d) FT-IR spectra of PVC 40 wt% DPE-SNa and FT-IR spectra of PVC 80 wt% DPE-SNa.

of  $-\text{CH}=\text{CH}-$ , as seen from Fig. 3(b), but no peak at 5.78 ppm was detected in the  $^1\text{H}$  NMR spectra of DDPE, DTPE, and DTDPE (Song et al., 2020; Ma et al., 2020; Won et al., 2018; Huang et al., 2018). In addition, new peaks appeared at 2.65 ppm, which were attributed to the protons of  $-\text{CH}_2-$  derived from thiol segment. The results showed that DDPE, DTPE, and DTDPE were obtained.

DPE-SH was synthesized through thiol-ene click reaction. Fig. 2(c) shows the FT-IR spectra of DPE, DPE-SH, and DPE-SNa. The infrared characteristic absorption peak of  $-\text{CH}=\text{CH}-$  was observed at  $1610\text{ cm}^{-1}$  in the FT-IR spectrum of DPE, but no peak was detected in the FT-IR spectrum of DPE-SH. The peak at 5.78 ppm in the  $^1\text{H}$  NMR spectrum of DPE was attributed to the protons of  $-\text{CH}=\text{CH}-$ , as shown in Fig. 3(c). However, no peak was detected at 5.78 ppm in the  $^1\text{H}$  NMR spectrum of DPE-SH. The results showed that thiol-ene click reaction was completed (Song et al., 2020; Ma et al., 2020; Won et al., 2018; Huang et al., 2018). The FT-IR spectrum of DPE-SNa showed a new peak at  $3362\text{ cm}^{-1}$ , compared with that of DPE-SH. The peak was attributed to  $-\text{SNa}$ . The  $^1\text{H}$  NMR spectrum of DPE-SH was similar to that of DPE-SNa.

The internally plasticized PVC (PVC 40 wt% DPE-SNa and PVC 80 wt% DPE-SNa) were investigated and compared with PVC. The results are shown in Fig. 2(d) and Fig. 3(d), the peaks at  $1733\text{ cm}^{-1}$  and  $1513\text{ cm}^{-1}$  in the FT-IR spectra of PVC 40 wt% DPE-SNa and PVC 80 wt% DPE-SNa corresponded to  $\text{C}=\text{O}$  and benzene ring derived from DPE-SNa, respectively. New peaks appeared at 6.6–6.7 ppm in the  $^1\text{H}$  NMR spectra of PVC 40 wt% DPE-SNa and PVC 80 wt% DPE-SNa, corresponding to the protons of  $\text{C}_6\text{H}_3$  derived from DPE-SNa. All the results showed that PVC 40 wt% DPE-SNa and PVC 80 wt% DPE-SNa were successfully synthesized.

### 3.2. The thermal stability of plasticizers

The thermal degradation processes of DPE, DDPE, DTPE, and DTDPE were investigated through TGA. As shown in Fig. 4(a) and (b), DPE had the worst thermal stability at approximately  $40\text{--}400\text{ }^\circ\text{C}$ . As the number ester groups covalently linked to DDPE, DTPE, and DTDPE as terminal groups, thermal stability improved, that is, ester group was positively correlated with thermal stability at  $40\text{--}400\text{ }^\circ\text{C}$ . DPE, DDPE, DTPE, and

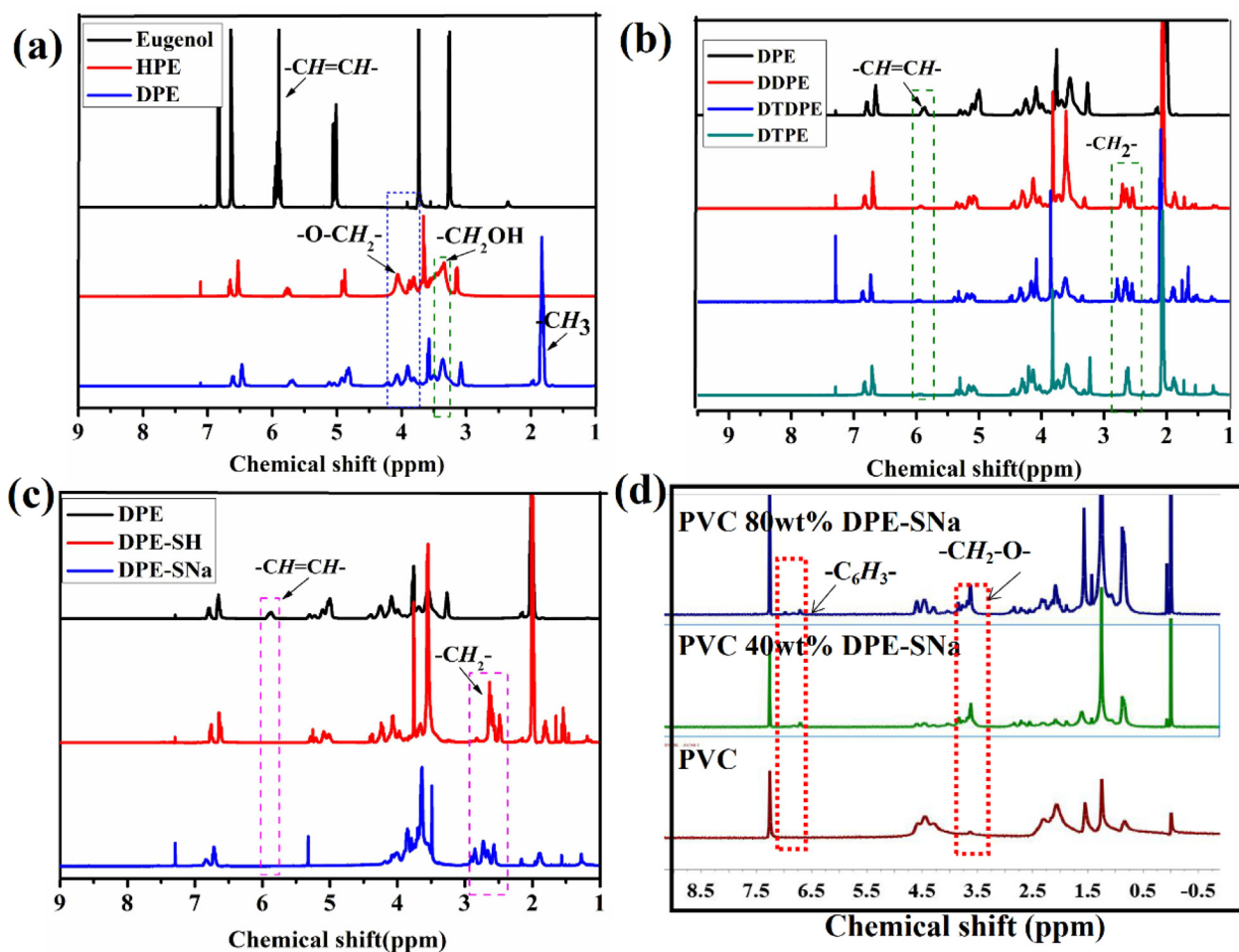


**Fig. 3** (a)  $^1\text{H}$  NMR spectra of eugenol, HEP and DPE (b)  $^1\text{H}$  NMR spectra of DDPE, DTPE and DTDPE (c)  $^1\text{H}$  NMR spectra of DEP, DPE-SH and DPE-SNa (d)  $^1\text{H}$  NMR spectra of PVC, PVC 40 wt% DPE-SNa and PVC 80 wt% DPE-SNa.

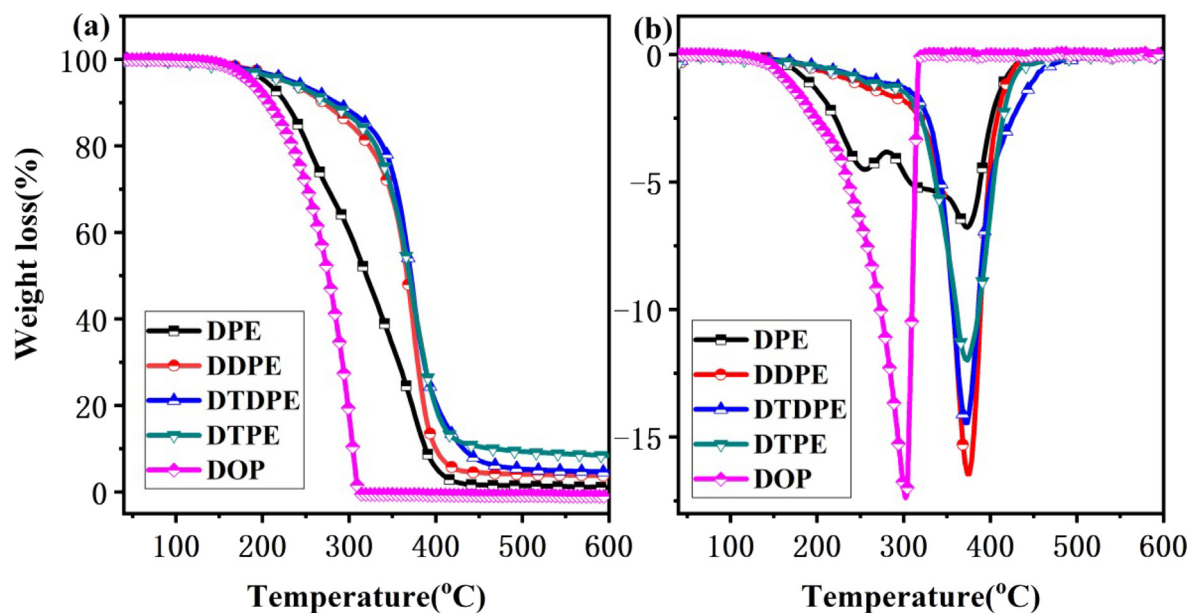


Fig. 4 (a) TGA curves of DPE, DDPE, DTPE and DTDPE.(b) DTG curves of DPE, DDPE, DTPE and DTDPE.

DTDPE showed better thermal stability than DOP (Ma et al., 2020). The results can be used as references for the design and synthesis of heat-resistant plasticizers.

### 3.3. The thermal stability of plasticized PVC

Thermal stability of plasticized PVC with DPE, DDPE, DTPE, or DTDPE was investigated through TGA. Fig. 5(a) and (b) show the thermal degradation curves of PVC and plasticized PVC. The degraded temperatures of plasticized PVC were higher than the control PVC sample, indicating that DPE, DDPE, DTPE, and DTDPE improved the thermal stability of plasticized PVC. The possible reason was the presence of a large number of ester groups with high heat resistance in the structures of DPE, DDPE, DTPE, and DTDPE. In addition, as the number of ester groups covalently attached to the chemical structure of plasticizer increased, such as DTPE, the plasticized PVC presented higher thermal stability compared with other samples. The internally plasticized PVC (PVC 40 wt% DPE-SNa and PVC 80 wt% DPE-SNa) were studied through TGA. As shown in Fig. 5(c) and (d), the thermal stability of the internally plasticized PVC was worse than PVC because of the thermal instability of C—S—C bonds.

### 3.4. The toxicity of plasticizers

The toxicity of DPE, DDPE, DTPE, and DTDPE was studied at 5000 mg/kg. There is not any death occurred among the test animals during acute oral toxicity tests, which indicated that all branched plasticizers (DPE, DDPE, DTPE, and DTDPE) were nontoxic plasticizers at a dose of 5000 mg/kg of body weight.

### 3.5. The microstructures of plasticized PVC

The microstructures of plasticized PVC and neat PVC were investigated through metallurgical microscopy. The results are shown in Fig. 6 and Fig. S4. As shown in Fig. S3,

the microstructure of PVC contained many agglomerates. An interesting phenomenon was that the number of agglomerates was positively correlated with the relative molecular weight of a plasticizer and the number of ester groups. The microstructure of PVC 40 wt% DPE (Fig. 6a) showed lower number of small agglomerates causing by the intermolecular interaction of carbonyl group of DPE and  $\alpha$ -hydrogen of PVC (Fig. S5). These interactions promoted mutual dissolution between PVC resin and DPE partly or completely, further causing the disappearance of the boundary in the PVC matrix. However, numerous agglomerates appeared in the microstructure of PVC 40 wt% DTPE because of intertwined PVC chains, which was generated because the interactions of carbonyl groups of DTPE and  $\alpha$ -H of the PVC was weaker than the same interactions in DPE (Suresh et al., 2018). These weak interactions promoted mutual dissolution between the PVC resin and DTPE partly or completely, which caused the intertwining of PVC chains. In the internally plasticized PVC (PVC 40 wt% DPE-SNa and PVC 80 wt% DPE-SNa), the microstructure of the materials showed many cracks and agglomerates owing to the intertwining of internal PVC chains. DPE units were chemically attached to PVC chains, and thus the mutual dissolution between PVC resin and DPE units was inhibited.

Mode of plasticization was investigated according to 2D and 3D AFM of PVC films. The results are shown in Fig. 7. The roughness factor (Rq) of 2D AFM of PVC 40 wt% DPE were 6.781. The average surface roughness (Ra) value was 9.147 nm. These data were lower than the values in PVC 40 wt% DTPE (Ra = 11.290; Rq = 13.108) and PVC 80 wt% DPE-SNa (Ra = 21.321; Rq = 24.110), indicating that the surface of PVC 80 wt% DPE-SNa was rough. The 3D AFM of PVC 40 wt% DPE showed less peaks than other samples. The phenomenon can be explained by compatibility theory. The intertwining of PVC 80 wt% DPE-SNa caused an irregular surface. PVC was more easy to dissolve in DPE than DTPE, which caused improved surface structure and flexibility of PVC 40 wt% DPE.

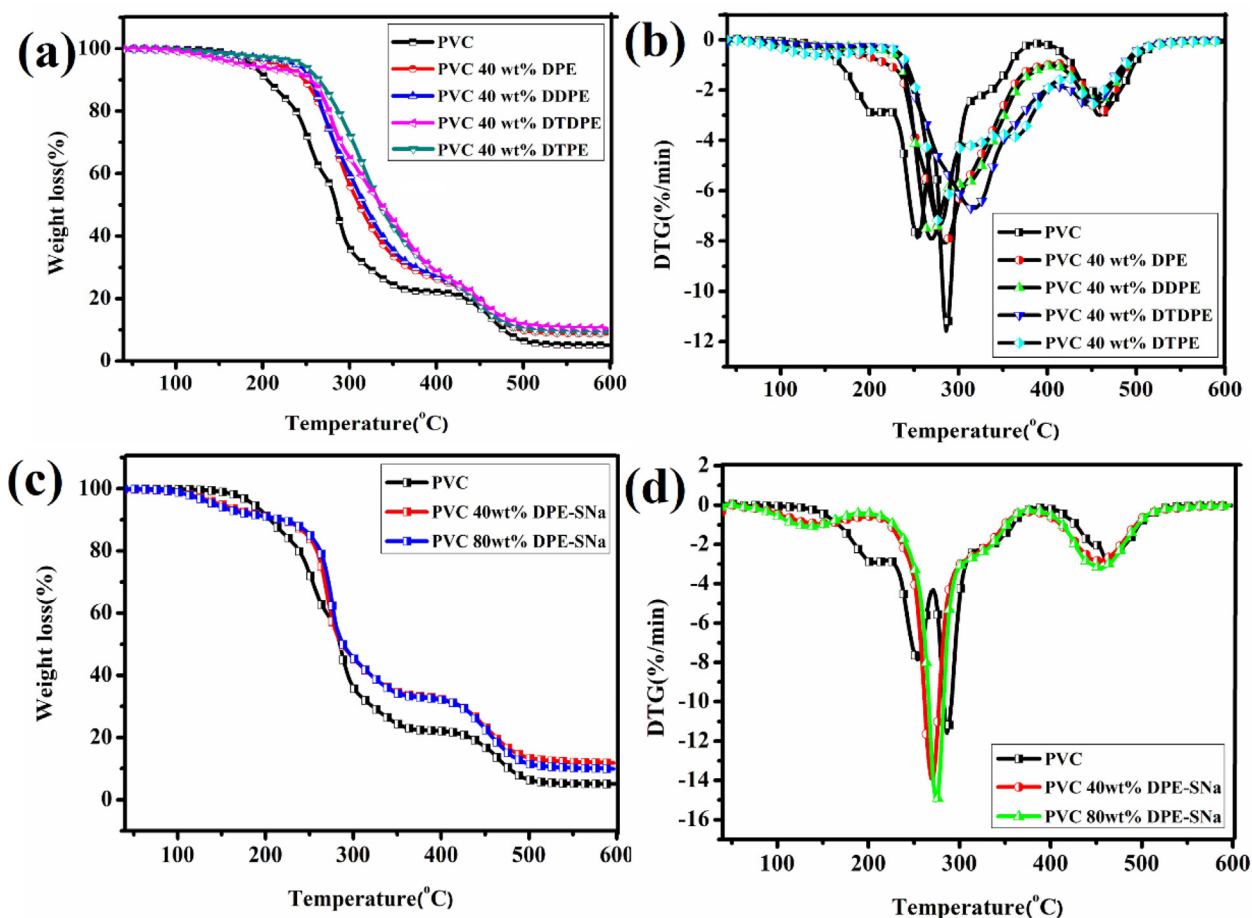


**Fig. 5** (a) TGA curves of plasticized PVC with DPE, DDPT, DTPE and DTDPE (b) DTG curves of plasticized PVC with DPE, DDPT, DTPE and DTDPE (c) TGA curves of internally plasticized PVC (d) DTG curves of internally plasticized PVC.

### 3.6. Glass transition and tensile properties of plasticized PVC compositions

$T_g$  of PVC materials can be reduced by blending with plasticizer (Najafi and Abdollahi, 2020).  $T_g$  of pure PVC is around 80 °C (Ma et al., 2020; Earla et al., 2017; Xu et al., 2004; Liu et al., 2006). The plasticizing effect of DPE, DDPT, DTPE, and DTDPE on PVC was evaluated according to the reduction in  $T_g$ . Only one  $T_g$  can be found for these PVC materials (Fig. 8[a]), which illustrated that PVC and plasticizers (DPE, DDPT, DTPE, and DTDPE) are compatible. The  $T_g$  values of plasticized PVC materials with DPE, DTDPE, DDPE, or DTPE were  $-0.7$  °C,  $2.7$  °C,  $5.6$  °C, and  $15.7$  °C, respectively. The results showed that the numerous ester groups and benzene rings played cooperative plasticizing effects on the PVC matrix. The benzene ring containing a plasticizer with a low degree of branching and low relative molecular mass exerted an excellent plasticizing effect on the PVC. Therefore, DPE was superior to other eugenol-based plasticizers in terms of plasticizing efficiency. In internally plasticized PVC materials, the  $T_g$  values of PVC 40 wt% DPE-SNa and PVC 80 wt% DPE-SNa were  $48.2$  °C and  $36.5$  °C (Fig. 8[b]), which were lower than the  $T_g$  value of PVC but were higher than plasticized the  $T_g$  values of PVC materials with DPE, DTDPE,

DDPE, or DTPE. The results showed that internal plasticizing efficiency was lower than the external plasticizing efficiency.

The tensile tests of PVC films are shown in Fig. 9(a) (b) and Table S1. The tensile strength and elongation at break of neat PVC are 32.33 MPa and 170 % (Ma et al., 2020). The flexibility of PVC 40 wt% DPE was the best. The strain and stress of PVC 40 wt% DPE were 13.2 MPa and 318 %, respectively. PVC 40 wt% DDPE, DTDPE, and DTPE showed gradual decrease in flexibility. The stress and strain of PVC 40 wt% DTPE were 24 MPa and 230 %. The results showed that DPE had higher plasticizing efficiency than DDPE, DTDPE, and DTPE. The tensile stress and tensile strain of internally plasticized PVC were investigated. As shown in Fig. 9(b), the flexibility of PVC 80 wt% DPE-SNa was higher than that of PVC 40 wt% DPE-SNa. However, the flexibility of the internally plasticized PVC was weaker than that of externally plasticized PVC.

### 3.7. The migration resistance of plasticized PVC

The migration resistance of PVC materials was evaluated. The results are shown in Fig. 9(c) and (d). As shown in Fig. 9(c), the weight loss rates of PVC 40 wt% DPE, PVC 40 wt% DDPE, PVC 40 wt% DTDPE, and PVC 40 wt% DTPE were

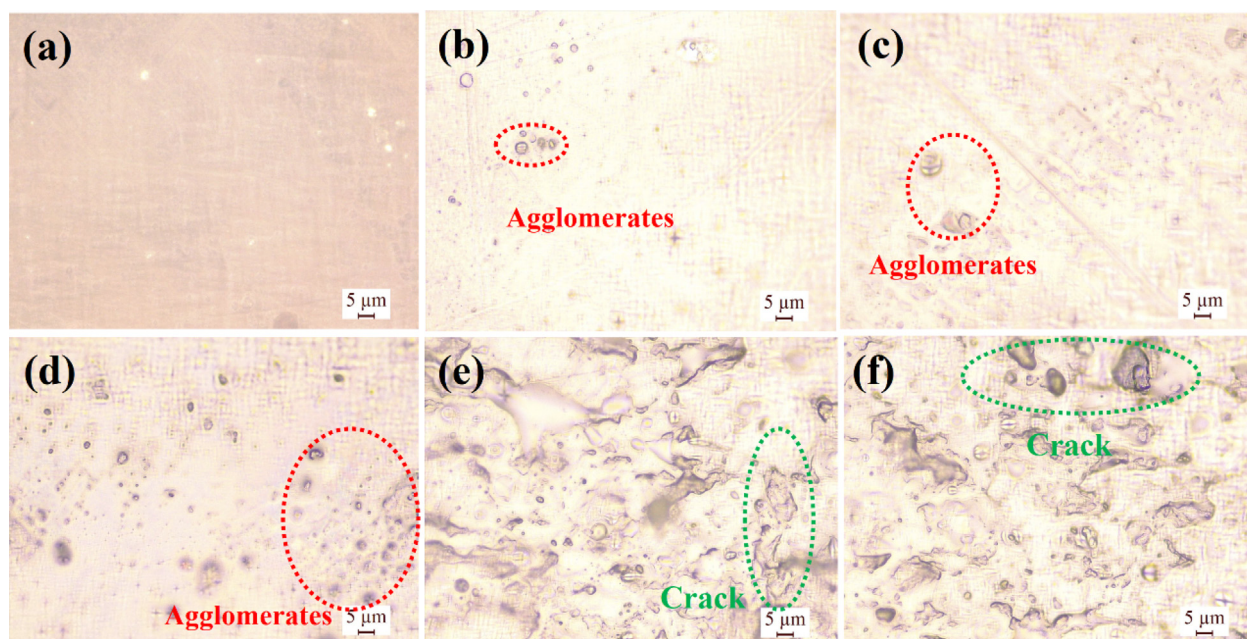


**Fig. 6** (a) Microstructure of PVC films plasticized with DPE (b) Microstructure of PVC films plasticized with DDPE (c) Microstructure of PVC films plasticized with DTDPE (d) Microstructure of PVC films plasticized with DTPE (e) Microstructure of PVC 40 wt% DPE-SNa films (f) Microstructure of PVC 80 wt% DPE-SNa films.

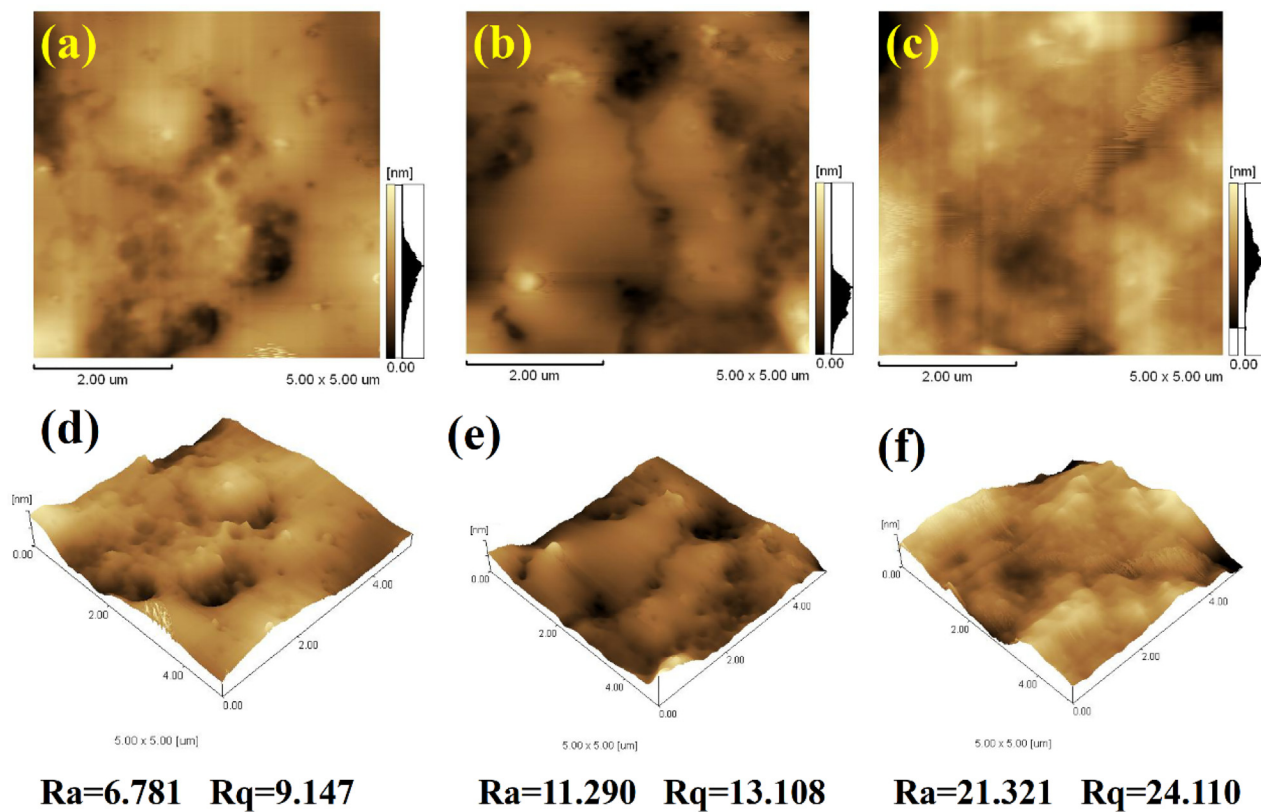


**Fig. 7** (a) 2D AFM of PVC 40 wt% DPE (b) 2D AFM of PVC 40 wt% DTPE (c) 2D AFM of PVC 80 wt% DPE-SNa (d) 3D AFM of PVC 40 wt% DPE (e) 3D AFM of PVC 40 wt% DTPE (f) 3D AFM of PVC 80 wt% DPE-SNa.

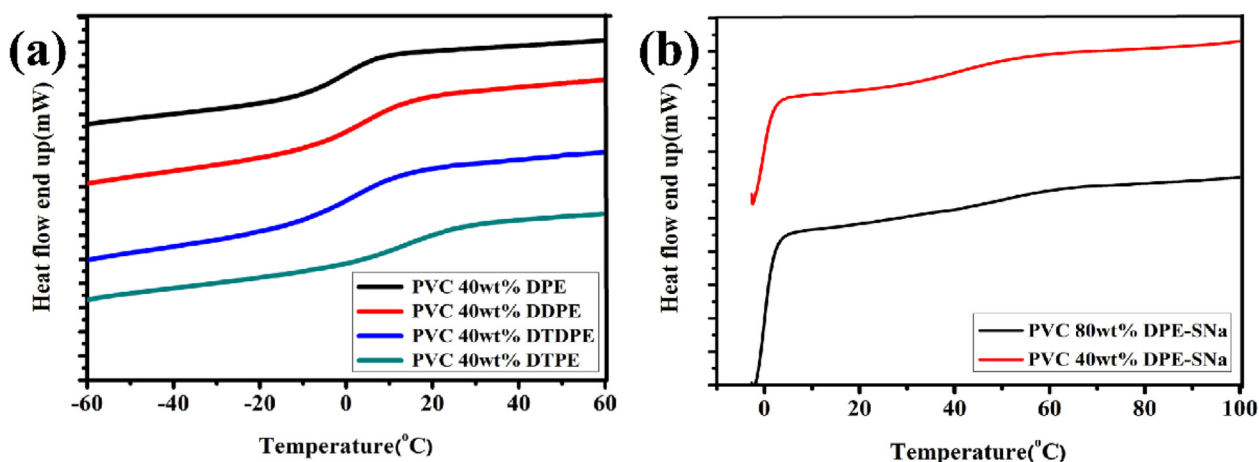


**Fig. 8** (a) DSC curves of plasticized PVC with DPE, DTDPE, DDPE and DTPE (b) DSC curves of internally plasticized PVC (c) DSC curves of plasticized PVC with DPE, DTDPE, DDPE and DTPE.

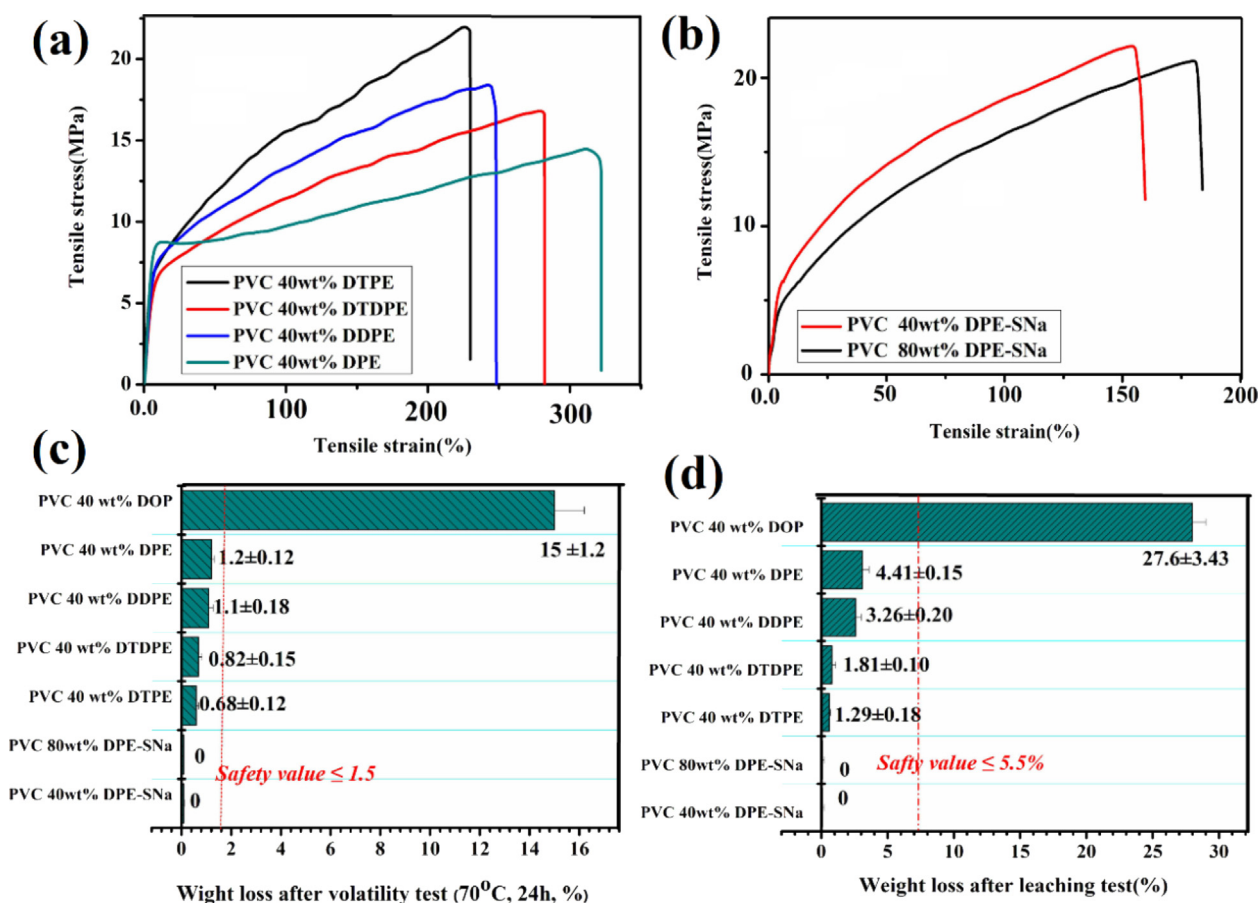


**Fig. 9** (a) Tensile strain-tensile stress of plasticized PVC with DTPE, DTDPE, DDPE and DTPE. (b) Tensile strain-tensile stress of internally plasticized PVC (c) Volatile resistance test of PVC films. (d) Solvent extraction resistance test of PVC films.

1.20 % ± 0.12 %, 1.10 % ± 0.18 %, 0.82 % ± 0.15 %, and 0.67 ± 0.12 lower than the safety value of 1.5 % (Tan et al., 2019; Tan et al., 2019). The weight loss of PVC/40phr DOP is 15 ± 1.25 (Ma et al., 2020), which illustrated that DPE, DDPE, DTDPE, and DTPE showed better migration resistance than DOP. Internally plasticized PVC materials, such

as 40 wt% DPE-SNa and PVC 80 wt% DPE-SNa, showed zero weight loss. The solvent resistance extraction results are showed in Fig. 9(d), the weight loss of PVC 40 wt% DPE, PVC 40 wt% DDPE, PVC 40 wt% DTDPE, and PVC 40 wt % DTPE were 4.41 % ± 0.15 %, 3.26 % ± 0.20 %, 1.81 % ± 0.10 %, and 1.26 % ± 0.18 %. The migration

stability was below the limit 5.5 % (Tan et al., 2019; Tan et al., 2019). Weight loss in PVC/40phr DOP was 27.6 %  $\pm$  3.43 %, which was extremely high (Ma et al., 2020). The results indicated that the durability of DPE, DDPE, DTDPE, and DTPE was superior to that of DOP. In addition, internally plasticized PVC materials, including 40 wt% DPE-SNa and PVC 80 wt% DPE-SNa, showed zero weight loss in the leaching test, which indicated that the migration resistance of 40 wt% DPE-SNa and PVC 80 wt% DPE-SNa was superior to that of externally plasticized PVC.

#### 4. Conclusions

Chemical conversion was successfully realized in eugenol derived from the waste residues of the rosin-processing industry to nontoxic plasticizers. Four kinds of sustainable branched plasticizers (DPE, DDPE, DTDPE, and DTPE) were synthesized based on a biomass resource, eugenol, through green polymerization and used to plasticize PVC. PVC modified with DPE-SNa was used to prepare internally plasticized PVC. Thermal stability of plasticized PVC with DPE, DDPE, DTDPE, or DTPE was enhanced. Thermal stability of the PVC modified with DPE-SNa was lower than that of PVC. The  $T_g$  values of plasticized PVC materials with DPE, DTDPE, DDPE, and DTPE were  $-0.7$  °C,  $2.7$  °C,  $5.6$  °C, and  $15.7$  °C, respectively. The plasticizing efficiency of DPE was superior to the other branched plasticizers. The  $T_g$  values of PVC 40 wt% DPE-SNa and PVC 80 wt% DPE-SNa were  $48.2$  °C and  $36.5$  °C, which were lower than the  $T_g$  value of PVC but were higher than the  $T_g$  values of plasticized PVC materials with DPE, DTDPE, DDPE, or DTPE. PVC 40 wt% DPE, PVC 40 wt% DDPE, PVC 40 wt% DTDPE, and PVC 40 wt% DTPE in the volatility and leaching tests showed safety value. Internally plasticized PVC materials, including 40 wt% DPE-SNa and PVC 80 wt% DPE-SNa, showed zero weight loss in the leaching test. The results indicated that the migration stability of internally plasticized PVC was higher than that of externally plasticized PVC. All the branched plasticizers were nontoxic plasticizers at a dose of 5000 mg/kg of body weight. All the sustainable branched plasticizers have potential application for plastic products, and the high-value utilization of the waste residues of the rosin-processing industry has numerous benefits.

#### CRedit authorship contribution statement

**Yun Hu:** Methodology, Formal analysis, Writing – review & editing. **Yufeng Ma:** Methodology, Formal analysis. **Jing Zhou:** Methodology, Formal analysis, Writing – review & editing. **Yu Bei:** Resources, Methodology. **Feilong Hu:** Methodology. **Zhimin Kou:** Investigation, Methodology. **Yonghong Zhou:** Resources, Supervision. **Puyou Jia:** Writing – review & editing, Supervision, Funding acquisition.

#### Declaration of Competing Interest

The authors declare that they have no known competing financial interests or personal relationships that could have appeared to influence the work reported in this paper.

#### Acknowledgments

This work was supported by the the Fundamental Research Funds of CAF (CAFYBB2022XB001), Guangxi Key Laboratory of Chemistry and Engineering of Forest Products (GXFK2203), and the Natural Science Foundation of Jiangsu Province (BK20201128).

#### Appendix A. Supplementary material

Supplementary data to this article can be found online at <https://doi.org/10.1016/j.arabjc.2022.104331>.

#### References

- Antti, S.J., Mikkala, V., Jonne, U., Henrikki, L., 2018. Effect of plasticizers on the mechanical and thermomechanical properties of cellulose-based biocomposite films. *Ind. Crops Prod.* 122, 513–521.
- Demircan, G., Kisa, M., Ozen, M., Aikgz, A., Kurt, M.A., 2020. A bio-based epoxy resin from rosin powder with improved mechanical performance. *Emerging Mater. Res.* 9, 1076–1081.
- Dumas, L., Bonnaud, L., Olivier, M., Poorteman, M., Dubois, P., 2015. Bio-based high performance thermosets: Stabilization and reinforcement of eugenol-based benzoxazine networks with BMI and CNT. *Eur. Polym. J.* 67, 494–502.
- Earla, A., Li, L., Costanzo, P., Braslau, R., 2017. Phthalate plasticizers covalently linked to PVC via copper-free or copper catalyzed azide-alkyne cycloadditions. *Polymer* 109, 1–12.
- Faye, I., Decostanzi, M., Ecochard, Y., Caillol, S., 2017. Eugenol bio-based epoxy thermosets: from cloves to applied materials. *Green Chem.* 19, 5236–5242.
- Fu-Lan, L.I., Yan, J., 2011. Preparation and Performance Testing of Porous NIPA Series Gels. *Technol. Develop. Chem. Ind.* 40, 17–21.
- Harvey, B.G., Sahagun, C.M., Guenther, A.J., Groshens, T.J., Cambrea, L.R., Reams, J.T., Mabry, J.M., 2014. A high-performance renewable thermosetting resin derived from eugenol. *ChemSusChem* 7, 1964–1969.
- Harvey, B.G., Guenther, A.J., Lai, W.W., Meylemans, H.A., Lamison, K.R., 2015. Effects of o-Methoxy Groups on the Properties and Thermal Stability of Renewable High-Temperature Cyanate Ester Resins. *Macromolecules* 48, 3173–3179.
- He, W., Zhu, G., Gao, Y., Wu, H., Guo, K., 2019. Green plasticizers derived from epoxidized soybean oil for poly (vinyl chloride): Continuous synthesis and evaluation in PVC films. *Chem. Eng. J.* 380, 122532.
- Howell, B.A., Lazar, S.T., 2019. Biobased Plasticizers from Glycerol/Adipic Acid Hyperbranched Poly(ester)s. *Ind. Eng. Chem. Res.* 58, 17227–17234.
- Hu, Y., Liu, C., Shang, Q., Zhou, Y., 2017. Synthesis and characterization of novel renewable castor oil-based UV-curable polyfunctional polyurethane acrylate. *J. Coat. Technol. Res.* 15, 77–85.
- Hu, Y., Feng, G., Shang, Q., Bo, C., Jia, P., Liu, C., Xu, F., Zhou, Y., 2018. Bio-based reactive diluent derived from cardanol and its application in polyurethane acrylate (PUA) coatings with high performance. *J. Coat. Technol. Res.* 16, 499–509.
- Huang, Y., Yu, E., Li, Y., Wei, Z., 2018. Novel branched poly( $\epsilon$ -caprolactone) as a nonmigrating plasticizer in flexible PVC: Synthesis and characterization. *J. Appl. Polym. Sci.* 135, 46542.
- Ji, S., Gao, C., Wang, H., Liu, Y., Hu, Z., 2019. Application of a bio-based polyester plasticizer modified by hydrosilicon-hydrogenation reaction in soft PVC films. *Polym. Adv. Technol.* 30, 1126–1134.
- Deng, J., Yang, B., Chen, C., Liang, J., 2015. Renewable Eugenol-based polymeric oil-absorbent microspheres: preparation and oil absorption ability. *ACS Sustainable Chem. Eng.* 3, 599–605.
- Kan, H., Wang, T., Yang, Z., Wu, R., Shen, J., Qu, G., Jia, H., 2020. High frequency discharge plasma induced plasticizer elimination in water: Removal performance and residual toxicity. *J. Hazard. Mater.* 383, 121185.
- Liu, W., Chul, K.H., Pak, P.K., Kim, J., 2006. C., Effect of acrylonitrile content on the glass transition temperature and melt index of PVC/SAN blends. *Fibers Polym.* 7, 36–41.
- Luo, Z.G., Liu, Z., Lin, J.Y., Wang, Q., Wan, C.R., 2012. Study on the application of catalytic esterification modification of rosin. *Adv. Mater. Res.* 430–432, 221–224.

- Ma, Y., Song, F., Hu, Y., Kong, Q., Jia, P., 2020. Highly branched and nontoxic plasticizers based on natural cashew shell oil by a facile and sustainable way. *J. Cleaner Prod.* 252, 119597.
- Mukherjee, S., Ghosh, M., 2020. Performance evaluation and biodegradation study of polyvinyl chloride films with castor oil-based plasticizer. *J. Am. Oil. Chem. Soc.* 97, 187–199.
- Nagai, S., Iwata, F., Kubo, K., 1977. Process for preparing o-alkoxy-p-allylphenols. US4048236 A.
- Najafi, V., Abdollahi, H., 2020. Internally plasticized PVC by four different green plasticizer compounds. *Eur. Polym. J.* 128, 109620.
- Silva, F., Monte, F., Lemos, T.D., Nascimento, P.D., Kelly, D., Paiva, L. D., 2018. Eugenol derivatives: synthesis, characterization, and evaluation of antibacterial and antioxidant activities. *Chem. Cent. J.* 12, 34.
- Sinisi, A., Degli Esposti, M., Toselli, M., Morselli, D., Fabbri, P., 2019. Biobased Ketal-Diester additives derived from levulinic acid: synthesis and effect on the thermal stability and thermomechanical properties of poly(vinyl chloride). *ACS Sustainable Chem. Eng.* 7, 13920–13931.
- Song, Y., Qiu, R., Hu, J., Li, X., Zhang, X., Chen, Y., Wu, W.-M., He, D., 2020. Biodegradation and disintegration of expanded polystyrene by land snails *Achatina fulica*. *Sci. Total Environ.* 746, 141289.
- Suresh, S.S., Mohanty, S., Nayak, S.K., 2018. Preparation of poly(vinyl chloride) / poly(methyl methacrylate) recycled blends: effect of varied concentration of PVC and PMMA in stability of PVC phase on the recycled blends. *Mater. Today: Proc.* 5, 8899–8907.
- Tan, J., Zhang, S., Lu, T., Li, R., Zhong, T., Zhu, X., 2019. Design and synthesis of ethoxylated esters derived from waste frying oil as anti-ultraviolet and efficient primary plasticizers for poly(vinyl chloride). *J. Cleaner Prod.* 229, 1274–1282.
- Tan, J., Lu, T., Li, R., Zhang, S., Zhu, X., 2019. Biodegradable waste frying oil-based ethoxylated esters as highly efficient plasticizers for poly(lactic acid). *ACS Sustainable Chem. Eng.* 7, 15957–15965.
- Teixeira, R.R., Gazolla, P., Silva, A., Borsodi, M., Bergmann, B. R., Ferreira, R.S., Vaz, B.G., Vasconcelos, G.A., Lima, W.P., 2018. Synthesis and leishmanicidal activity of eugenol derivatives bearing 1,2,3-triazole functionalities. *Eur. J. Med. Chem.* 146, 274–286.
- Trita, A.S., Over, L.C., Pollini, J., Baader, S., 2017. Synthesis of potential bisphenol A substitutes by isomerising metathesis of renewable raw materials. *Green Chem.* 19, 3051–3060.
- Wan, J., Gan, B., Li, C., Molina-Aldareguia, J., Kalali, E.N., Wang, X., Wang, D.Y., 2016. A sustainable, eugenol-derived epoxy resin with high biobased content, modulus, hardness and low flammability: synthesis, curing kinetics and structure-property relationship. *Chem. Eng. J.* 284, 1080.
- Wilkes, C.E., Summers, J.W., Daniels, C.A., Berard, M.T., 2005. *PVC handbook*. Hanser Munich 184.
- Won, L.K., Woo, C.J., Seung-Yeop, K., 2018. Highly branched polycaprolactone/glycidol copolymeric green plasticizer by one-pot solvent-free polymerization. *ACS Sustainable Chem. Eng.* 6, 9006–9017.
- Xu, Y., Gye, M.C., 2018. Developmental toxicity of dibutyl phthalate and citrate ester plasticizers in *Xenopus laevis* embryos. *Chemosphere* 204, 523–534.
- Xu, W.B., Zhou, Z.F., Ge, M.L., Pan, W.P., 2004. Polyvinyl Chloride/Mmontmorillonite Nanocomposites Glass transition temperature and mechanical properties. *J. Therm. Anal. Calorim.* 78, 91–99.
- Xuan, W., Hakkarainen, M., Odellius, K., 2019. Levulinic acid as a versatile building block for plasticizer design. *ACS Sustainable Chem. Eng.* 7, 12552–12562.
- Zhu, H., Yang, J., Wu, M., Wu, Q., Liu, J., Zhang, J., 2021. Biobased plasticizers from tartaric acid: synthesis and effect of alkyl chain length on the properties of poly(vinyl chloride). *ACS Omega* 6, 13161–13169.